Coordination Chemistry Reviews
182 (1999) 343–371

Strains and stresses in coordination compounds

Peter Comba *

Anorganisch-Chemisches Institut, Universität Heidelberg, Im Neuenheimer Feld 270,
69120 Heidelberg, Germany

Received 1 May 1998

Contents

Abstract

The possible ways to induce strain in coordination compounds and the quantification of steric effects and their influence on molecular properties are discussed. Based on various

---

* Tel.: +49-6221-548453; Fax: +49-6221-546617; e-mail: comba@akcomba.oci.uni-heidelberg.de.

PII: S0010-8545(98)00199-4

specific examples, including cobalt(III), cobalt(II), iron(III) and iron(II) hexaamines and copper(II) and copper(I) tetraamines, observed and computed structural data are used to analyze the effects of extremely short and long bonds and of severe angular distortions on reactivities, complex stabilities, electronic and EPR spectra and reduction potentials. Methods that allow the prediction of these molecular properties, based on experimentally determined or computed structures, are described in detail.

Keywords: Ligand field; Reduction potential; Preorganization; Entatic state; Hexaamine; Steric effects; Steric strain; Catalysis; Molecular modeling

1. Introduction

The coordination of ligand molecules to a metal ion generally leads to stress and strain. Stress refers to the interactions between atoms in a molecule that lead to distortion and, consequently, to destabilization; strain is the deformation in a molecule that results from stresses.

The structure of a coordination compound is the result of a compromise between all stresses involving interactions within the ligand backbones and between the ligand molecules and the metal center. Therefore, the structure of a coordination compound is the result of a compromise between metal ion and ligand dictation. In general, bond distances and valence angles involving carbon atoms are much stiffer than those involving metal ions, i.e. coordination geometries are variable to a larger extent than bond distances and valence angles within the ligand backbone. The main degrees of freedom within a ligand backbone to accommodate metal ion preferences are conformational rearrangements, that is, variations of torsional angles. It follows that, in order to enforce a particular coordination geometry, the conformational freedom needs to be restricted by multiple bonds, sterically demanding substituents or by ring systems. The plasticity of transition metal ion coordination centers is, to a large extent, the result of the bonding that involves partly filled d-orbitals of the metal center. Ligand enforced variation of the coordination geometry leads to changes of the thermodynamic, kinetic and electronic properties, that is, to a variation of stabilities, reactivities and spectroscopic properties. Thus, there are two important consequences of enforcing specific ligand and coordination geometries[1]: activation and preorganization i.e. catalysis and selectivity.

1.1. Preorganization

The structure of a preorganized metal-free ligand is identical to that of the corresponding coordinated ligand [1,2], i.e. upon coordination there is no strain induced to the ligand by the metal center and no strain to the metal center by the

---

[1] Similar principles apply to other areas of chemistry; in this report, I concentrate on classical coordination chemistry.

ligand. It follows that preorganization refers to a particular ligand/metal ion pair and that preorganized ligands are relatively rigid. Deviation from full preorganization leads to destabilization of the complex by the amount of strain induced by the complexation reaction. Based on computed structures and strain energies, the degree of preorganization of a ligand has been defined and quantified [3]. This concept may be used to predict the loss of steric energy during the complexation reaction when a particular ligand does not fully fit the requirements of the metal ion, and it emerges that stresses which are built into the ligand backbone may reduce the strain accompanying the complexation reaction (i.e. the strain is already present in the metal-free ligand). This is a concept that resembles that of the entatic state principle discussed in relation with metal complex based catalysis (see below). A number of approaches, primarily based on molecular mechanics calculations, have been used to predict the preorganization and metal ion selectivity of ligand systems, and these have been reviewed extensively [3–14]. Note that steric effects are not the only components responsible for complex stabilities (and reactivities), and effects based on metal ion–donor atom orbital overlap are not usually fully included in the strain of the metal–donor bonds, the angular strain around the metal ion and that around the donor atom (see Section 2.2).

Stereoselectivity involving coordination compounds is another prominent area where ligand-based stresses are an important factor, and this may generally be interpreted on the basis of the key–lock principle [15]. Examples include racemate separations based on outer-sphere interactions [16–20] and on ligand exchange reactions [21–24], and metal complex catalyzed stereoselective syntheses [25–28]. The basis generally is that there is a difference in strain energy between the two diastereomeric forms of the complex between the optically pure chiral matrix (coordination compound or complex fragment) and the substrate. Depending on the type of structure responsible for the stereoselectivity (racemate separation or enantioselective catalysis; thermodynamic or kinetic effect; inert or labile product; ground state or transition state) there are relatively simple or more elaborate methods to quantify the strain energy differences and interpret or predict the stereoselectivity, i.e. the computation of transition states and of bond breaking and bond making requires more elaborate techniques [8,29–32].

1.2. Catalysis

Catalysis is the selective activation of a reaction path by reduction of the corresponding activation energy. The energy difference between the starting materials and the transition state may be decreased by either stabilization of the transition state and/or by destabilization of the starting materials. The latter is known as the rack- or entatic state approach [33,34]. Often, metalloproteins operate in the entatic state mode or a variant, i.e. the induced fit mode [35,36], and in a number of industrially important processes the catalysts are strained metal complexes.

The long term stability of a catalyst is an important requirement that may be decisive in terms of industrial applications. Thus, the selective activation of a reaction path by a destabilization of the catalyst/substrate complex with rigid rings and sterically demanding substituents in the ligand backbone of the catalyst may lead to serious problems. However, in the catalytic cycle, there usually is also the necessity for a fast complexation/decomplexation reaction between the catalyst and the substrate, i.e. the catalyst–substrate bond needs to be labile. The protein backbone in metalloproteins is responsible for both, the deformation of the active site chromophore and the overall stability of the active site. Substrate binding may occur at particular coordination sites that are not protected by the protein backbone and amino acid side chains; cooperative effects may help to channel the substrate to the active site; particular side chains may help to stabilize the enzyme–substrate complex e.g. by hydrogen bonding. The tools of preparative chemists to deal with these factors in low molecular weight catalysts include the stabilization of the coordination compound by chelating and macrocyclic ligands, partial shielding of the metal center by the ligand backbone; the induction of strain by sterically demanding groups and fused ring systems.

2. Structure and strain

2.1. Ideal geometries

Before discussing strained, distorted structures it is appropriate to reflect the problem of defining ideal, undeformed, unstrained geometries. In general, ideal geometries (undeformed distances and angles) are not experimentally observable. There are always stresses in molecules, and each observed structural parameter is the result of a compromise that involves the minimization of all these stresses. That is, basically each structural parameter in any real molecule is strained to some extent. Ideal valence angles (for example sp, sp^2 and sp^3, i.e. 180, 120, 109°), ideal torsional angles and the planarity of aromatic rings, for example, are, to a large extent, indisputable (less evident is the energetic penalty upon distortion). For other parameters, such as van der Waals radii and, specifically, for ideal bond distances, there is no experimental or theoretical basis for the definition of unique, accurate and unambiguous parameter values [8].

Consider, for example, hexaamine cobalt(III) compounds (Table 1). The average $Co^{III}–N$ distance is ca. 1.97 Å and the mean N–Co–N valence angle is close to the expected 90 and 180°. A recent CCDC (Cambridge Crystallographic Data Center) search reveals that, even for low spin d^6 systems, which, due to the strong ligand field, are relatively rigid, the angular geometry is quite variable with maximum angular distortions of up to 20°. As expected, the variation in bond distances is less pronounced and, due to the anharmonicity of the bonding potential, the maximum variation to longer bonds is larger than the maximum variation to shorter bonds.

The question of whether long and short bonds are elongated or compressed, respectively, is dependent on the accurate definition of an ideal geometry and this has been discussed controversially in the literature [4,6,8,40–42]. The sterically least demanding ligands in series of similar ligand molecules have been assumed as reference points and, consequently, metal–donor distances shorter than these have been defined as compressed [4,6,41,42]. For example, NH_3 is the sterically least demanding amine, and cobalt(III)–amine distances < 1.965 Å might then be interpreted as compressed bonds. The Co^{III}–N bonds in $[Co(\textit{trans}\text{-diammac})]^{3+}$ (*trans*-diammac = *exo*-6,13-diamino-6,13-dimethyl-1,4,8,11-tetraazacyclotetradecane; for the structure and data see Chart 2, Table 6 and Fig. 3) are shorter than those in $[Co(NH_3)_6]^{3+}$ (1.946, 1.937 vs. 1.965 Å, see Table 6) and, as a result, $[Co(\textit{trans}\text{-diammac})]^{3+}$ has an extremely high ligand field and a strongly negative reduction potential (see Table 7) [43]. However, this does not necessarily indicate that these Co^{III}–N bonds are compressed, they are just short [8,40]. The computed Co^{III}–N distance in a complex with hypothetically bare amine nitrogen donors indicates that, in absence of repulsion due to hydrogen ‘substituents’ but without any stresses involving the ligand backbone (as might occur in macrocyclic ligand compounds) the Co^{III}–N bond might be very short indeed (see Table 1). Note, however, that this computed distance is very much dependent on the model and parameterization used. Here, this point is discussed to stress the problem of defining normal or ideal bond distances. As a matter of fact, the undeformed or ideal bond

Table 1
Hexaamine cobalt(III) coordination geometries

	Co–N (Å)				N–Co–N (°)			Source
	Average	Min	Max	σ	Average	Min	Max	
$Co(NH_3)_6^{3+}$	1.965	—	—	0.021	—	—	—	[37]
$Co(NH_2R)_6^{3+}$ [a]	1.965	—	—	0.021	—	—	—	[37]
$Co(NHR_2)_6^{3+}$ [a]	1.968	—	—	0.030	—	—	—	[37]
$Co(NR_3)_6^{3+}$ [b]	1.961	—	—	0.027	—	—	—	[37]
$Co(NR_3)_6^{3+}$ [c]	1.974	1.906	2.093	—	90, 176	72, 158	103	[d]
	Co–N (Å)							
	Exp.	MOMEC [38] [e]						
$Co(NH_3)_6^{3+}$	1.965	1.955						[8]
$Co(NH_2Me)_6^{3+}$ [f]	2.013	1.983						[8]
$Co(N)_6^{3+}$ [g]	—	1.933						[8]

[a] R = alkyl.

[b] R = any carbon substituent.

[c] R = H or alkyl.

[d] CCDC; sample: 175 structures.

[e] $k_b = 1.75$ mdyn Å^{-1}; $r_0 = 1.905$ Å.

[f] Experimental: [39].

[g] Hypothetical Co^{III}–N complex with six bare N donors (1,3-van der Waals interactions included).

Table 2
Variation of published ideal Co^{III}–N distances (r_0) and force constants (k_b)

r_0 (Å)	k_b (mdyn $Å^{-1}$)	Refs.
1.905	1.75	[44–46]
1.927	2.25	[47]
1.915	2.00	[47]
1.915	1.75	[47]
1.925	1.70	[48]
1.950	2.25	[49]

distances used in molecular mechanics force fields might be used as reference points. Inspection of Table 2 indicates, however, that the variation of ideal Co^{III}–N bond distances in molecular mechanics force fields that are used successfully in modeling hexaamine cobalt(III) compounds is too large to use these parameters as reference values for an undeformed cobalt(III)–amine nitrogen distance.

From Table 1, it emerges also that the cobalt(III)–amine bond distances are approximately independent of the type of the amine donor. That is, distances to ammonia, primary, secondary and tertiary amines are roughly identical. Due to inductive effects the nucleophilicity of amine donors is expected to increase with the number of alkyl substituents. Thus, the bond strength is expected to increase with an increasing number of alkyl substituents. The observed independence of Co^{III}–N bond lengths from the type of amine may be the result of two opposing effects, i.e. of increasing bond strength due to an increasing nucleophilicity and of bond elongation due to stresses induced by the substituents. A recent analysis based on quantum mechanical calculations and experimental data, which supports this interpretation, has been challenged on the basis of misinterpretations of the experimental data [50,51]. Our analysis of ligand field spectroscopic properties of transition metal compounds, based on a combination of molecular mechanics calculations (MM) for the optimization of the structures with angular overlap model calculations (AOM) for the computation of the d-electron energy levels (MM-AOM) [52–55], allows a separation of steric and electronic effects [56]. A

Table 3
MM-AOM—the nucleophilicity of substituted amines

	e_σ (norm) (cm^{-1})[a]		
	Cr^{III} (2.08 Å)	Co^{III} (1.98 Å)	Ni^{II} (2.13 Å)
NH_3	7200	7245	3582
RNH_2	7400	7433	3857
R_2NH	8000	7715	4133
R_3N	8700	8186	4592

[a] e_σ values are normalized to the M–N distances given in brackets; $e_\sigma = f(1/r^n)$, where r = M–N and $n = 6$.

careful analysis of the data (see Tables 1 and 3) indicates that, indeed, the observed independence of the Co^{III}–N distances from the number of amine alkyl substituents is the consequence of a compromise between bond strengthening due to increasing nucleophilicity and bond elongation due to steric strain [56]. Changes in nucleophilicity due to amine substitution have also been discussed in relation with our recently communicated results on the modeling of reduction potentials, based on force field calculations (MM-redox, see below) [31,57].

2.2. Strain

Stabilities, selectivities, reactivities and electronics depend on structures and, therefore, on strain and deformation. There are two problems in defining stresses and strain: (i) the accurate definition of relaxed reference structures (see Section 2.1) is a requirement for the quantification of strains and stresses. Also, the absolute value of stress and strain must be independent from the size of the molecule and, therefore, it requires some normalization. Generally, strain energies reported in the literature are relative energies, and they may therefore only be used for the interpretation of thermodynamics within a set of isomers [8]. (ii) what are the relevant terms for a discussion of stress and strain? An optimized structure will have stresses relaxed to the extent that the total free energy of the system (ΔG) is minimal. Therefore, strain involves classical steric terms such as non-bonded interaction energies (van der Waals attraction and repulsion, hydrogen bonding, electrostatic interactions), angular and torsional strain, as well as electronic terms (bond strengths and strains based on specific electronic effects, such as Jahn–Teller distortions, *trans*-influences, etc.), environmental effects (crystal lattice effects, ion pairing, solvation) and entropic effects i.e. there is strain based on non-bonded intramolecular interactions, there is electronic strain, strain based on intermolecular interactions and entropic strain. Depending on the type of study, some of these terms may be neglected, and this may restrict the applicability of the results, interpretations and conclusions.

Three interesting examples that may be related to electronic strain are shown in Figs. 1 and 2 and Table 4: in the first two examples the structures of the hexacoordinated copper(II) compounds are the result of a tetragonal distortion due to a Jahn–Teller lability. The complex stabilities shown in Fig. 1 may be interpreted as follows: the elongation of a trigonal $[Cu(en)_3]^{2+}$ (en = ethane-1,2-diamine, see Chart 2 below) chromophore along one of the Cartesian coordinate axes leads to a build up of strain within the ligand backbone that results in a destabilization of the corresponding tris-bidentate complex. The result is a deviation from the expected stability for M = Cu(II) (see Fig. 1) and, therefore, a deviation from the Irving-Williams series of complex stabilities [58,59].

The structure of $[Cu(hfacac)_2(bpy)]$ (hfacac = hexafluoroacetylacetonate; bpy = 2,2′-bipyridine) is a compromise that involves the Jahn–Teller lability of the d^9 electronic configuration of copper(II), the π-delocalization in the ligand backbones and the geometric requirements of the ligands and the metal center (see Fig. 2) [62]. A possible interpretation of the observed structure is that electronic strain (Jahn–

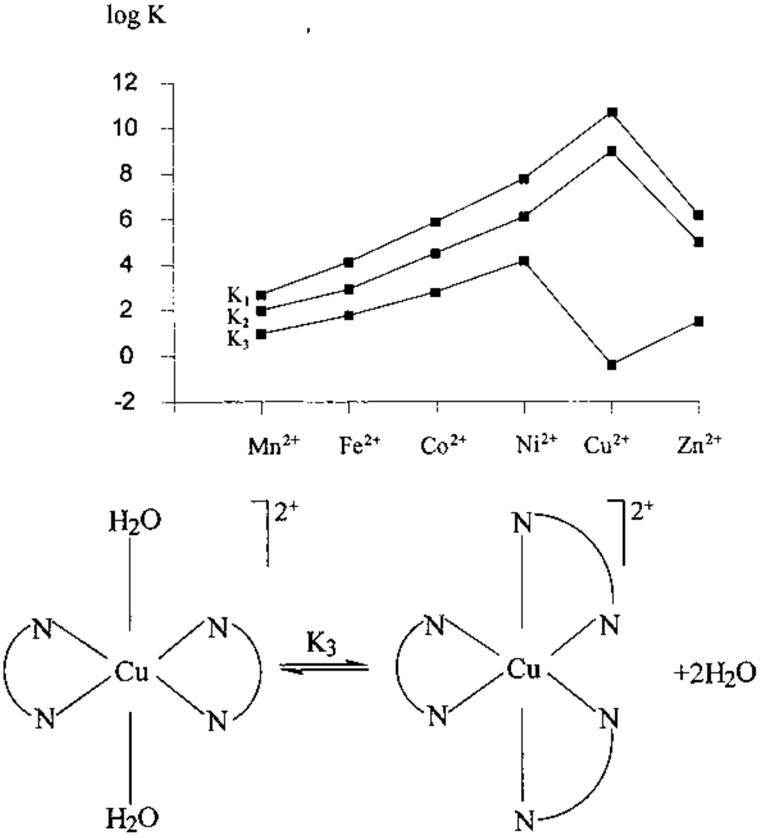

Fig. 1. Individual stability constants for the complexation of copper(II) with en [60,61].

Teller lability) leads to a build-up of steric strain in the hfacac ligand backbones that is relaxed by a loss of delocalization in the hfacac skeleton.

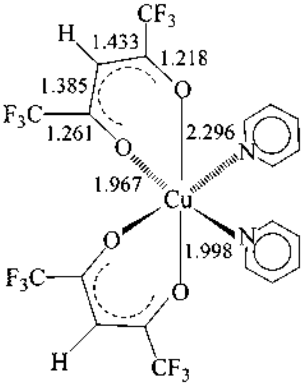

Fig. 2. Structure of [Cu(hfacac)$_2$(bpy)] (bond distances in Å) [62].

Table 4
Observed structural parameters of oxalate and M^{III} oxalato complexes[a,b,c]

	r_1 (Å)	r_2 (Å)	r_3 (Å)	r_4 (Å)	α (°)	β (°)	γ (°)	δ (°)	Plane[d]
Ti^{3+}	2.1	1.26	1.53	1.22	74.3	118.7	113.5	126.2	0.02 (0.13)
V^{3+}	2.0	1.27	1.54	1.21	80.3	115.5	114.1	125.8	0.0 (0.07)
Cr^{3+}	1.97	1.28	1.54	1.22	82.2	114.3	115.6	125.4	0.045 (0.0)
Mn^{3+}	2.00	1.28	1.56	1.22	80.9	115.6	113.6	126.8	0.05 (0.1)
Fe^{3+}	2.00	1.28	1.54	1.22	80.4	115.6	114.4	125.8	0.03 (0.16)
Co^{3+}	1.90	1.29	1.54	1.23	86.37	112.3	114.7	124.2	0.14 (0.07)
H_2ox	—	1.29	1.55	1.22	—	—	112.4	127	—
ox^{2-}	—	1.27	1.56	1.24	—	—	115.6	126.3	—

[a] For the definition of structural parameters see Chart 1.

[b] The data given are averages of all relevant distances and angles.

[c] For references to the experimental data see [46].

[d] R.M.S. deviation from the best plane of $C_2O_4^{2-}$ (Å) [distance of M from that plane (Å)].

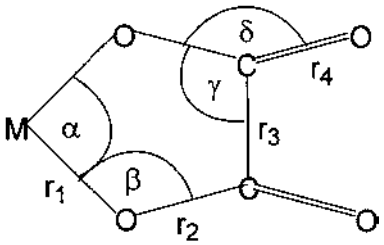

Chart 1.

In the two examples the structures are the result of opposing trends to minimize the energy. It emerges that, in cases where structures are the result of various factors (i.e. quite generally), there is not necessarily an unambiguous interpretation of the observed structure. A further example is the structural analysis of tris-oxalato complexes (see Table 4; the structural parameters are given in Chart 1) [46]: the most significant structural variation along the 3d row is a decrease of the M–O–C angle (β) from 119° (Ti^{III}, close to sp^2 hybridization) to 112° (Co^{III}, close to sp^3 hybridization). A possible interpretation is that the observed structural change is due to a decreasing π-donation of the carboxylate oxygen along the 3d series (increasing number of electrons in the t_{2g} π set of the d-orbitals of the metal center). Similar effects have been used to interpret structural, thermodynamic and kinetic data of coordinated $EDTA^{4-}$ type ligands ($EDTA^{4-}$ = ethylenediaminetetraacetate) [63]. An alternative interpretation of the data in Table 4 is that the M–O–C angle (β) is strongly correlated to the variation of M–O distances (r_1) and a concomitant increase in the bite angle (α).

3. Molecular modeling

Molecular modeling involves the optimization of molecular structures or of structures of arrays of molecules (crystal lattices, solvated molecules), the computation of the corresponding stabilities (free energies) and of electronic and spectroscopic properties (IR, EPR, NMR, UV–vis spectra, magnetic moments, etc.). Models used for structure optimization may be grouped in two classes: quantum mechanical and empirical force field calculations. Structural, thermodynamic and vibrational spectroscopic data may be directly obtained from both classes of models; electronic data are only directly available from quantum mechanical calculations. The main advantage of force field calculations (molecular mechanics) is that they are computationally less demanding. In the examples discussed below, molecular mechanics alone or in combination with other models and tools (for example ligand field calculations, spectra simulations, etc.) is used to compute structures and properties of coordination compounds. A number of recent reviews have described the theory and state of the art of molecular mechanics of coordination compounds [4,8,29,30,40,56,64–71] and that of molecular modeling in general, involving the combination of MM with various approaches for the computation of molecular properties (MM-isomer, MM-redox, MM-EPR, MM-AOM) [8,40,56,64–72]. For our own examples discussed below, the computer program and force fields for the molecular mechanics calculations [38,44–46] the program and parameter sets for the angular overlap model (AOM) calculations used in combination with MM (MM-AOM) [52–55,73–75], the program and technique used for EPR simulation in combination with MM (MM-EPR) [76–80] and the approach used for computing redox potentials (MM-redox) [31,57,81] have been tested thoroughly and described in detail elsewhere. The discussion here will be reduced to that of some basic principles.

3.1. Molecular mechanics

The basis of MM is that the energetics of a molecule or a molecular array may be described by the sum of all possible two atom interactions (bonds, van der Waals interactions, electrostatic interactions, hydrogen bonds), three atom interactions (angles), four and more atom interactions (proper and improper torsions), and that each of these potentials is independent of all the others or that simple terms exist that account for weak coupling between certain potentials. The ensemble of potential energy functions and their parameterization (the force field) allow to compute the energy (the strain energy) at each point of the potential energy surface, i.e. for each set of molecular coordinates that corresponds to a possible conformation, relaxed or distorted. Strain energy minimization algorithms search for the direction on the potential energy surface in which a set of coordinates with lower energy may be found.

There are examples, where the optimization of a structure is done with some internal coordinates (bonds, angles, torsions) fixed to specific values. This technique allows to map the potential energy surface along a conformational interconversion or to determine the strain induced by bond elongation or compression. The most precise method to constrain internal coordinates is by Lagrange multipliers, and this involves energy minimization by second derivative methods and the expansion of the

Hesse matrix of the second derivatives [82–86]. Recently, a new approach has been developed that allows one to constrain the sum of internal coordinates to specific values, while each individual coordinate is flexible [87]. This approach has been used to compute metal ion independent hole sizes of asymmetrical macrocyclic ligands, where the conventional approaches have been shown to lead to erroneous results [8]. The shape and the size of a metal-free ligand cavity may be an important feature related to preorganization and, therefore, to complex stability and metal ion selectivity [4,8]; various methods to compute hole sizes have been developed and the results and interpretations have been discussed controversially [6–8,14,40,88–91]. The intriguing problem here is that the computation of metal ion independent hole sizes involves the computation of stresses induced to the ligand by the metal center without any specific metal ion in the cavity (this problem is related to the fact that preorganization is a property of a specific metal ion/ligand pair, see above, i.e. it cannot be metal ion independent). Problems related to this contradictory situation and the general question of how significant and useful the concept of hole sizes is, have been discussed in detail on the basis of hole size computations with a number of different approaches [87].

One of the major difficulties of geometry optimization of transition metal compounds by empirical force field calculations is the large variety of coordination centers, coordination numbers and coordination geometries and their plasticity. Methods to account for specific electronic effects due to partly filled d-orbitals of the metal centers include the combination of quantum mechanical and molecular mechanical methods [92–94], force field based models that include general ligand field [29] or general valence bond [30] terms, and classical molecular mechanics models with specific functions to account for Jahn–Teller distortions, *trans*-effects, the d-orbital directionality and the redistribution of electron density in the ligand backbone due to its coordination to a metal ion [45,46,95].

3.2. Neglected terms

Entropic contributions to the free energy, other than statistical terms, are often neglected [8,40]. The neglect of entropic strain (see above) may lead to a deformation of a computed structure. That is, the shape of the potential energy surface may be inaccurate due to missing entropy terms. More importantly, the computed free energy differences between two isomers may be inaccurate due to the neglect of entropic terms. Experimental studies of the temperature dependence of isomer ratios and corresponding computations indicate that, at least for cobalt(III) hexaamines, the neglect of entropy does not lead to unacceptable inaccuracies [8,24,96–98]. The effect of neglecting entropic strain has also been discussed in recent publications on the computation of reduction potentials (and electron transfer rates) based on molecular mechanics calculations [31,57]. In general, for simple coordination compounds, the neglect of entropy does not lead to intolerable inaccuracies. Therefore, in the area of classical coordination compounds, there are only few reports where the classical partition functions for the computing of the entropy contributions to the free energy have been included in force field calculations[2] [8,96,99–101].

Interactions between isolated molecules and their environment (solvation, ion pairing, intermolecular hydrogen bonding and electrostatic effects) are often neglected in structural optimization procedures. There is no fundamental reason for this, since the corresponding potentials (primarily van der Waals, electrostatic and hydrogen bonding terms) and their parameterization are usually available; the only major problem here is the computation of the charge distribution but there are methods to deal with this potentially difficult task [8,102–106]. The simple reason for optimizing isolated molecules is the computational expense for the computing of crystal lattices and solvated and ion-paired molecules. Techniques to compute relatively large arrays of molecules are available [56,102,107–109]. Force fields that are based on experimental data (structural, vibronic spectroscopic or thermodynamic) from solutions or solids have interactions to and from the environment included in the parameter values, i.e. averaged interactions with the environment are included, and this has been discussed in detail in recent review articles [56,64,66]. One of the problems of neglecting long-range effects is that van der Waals, hydrogen bonding and electrostatic interactions decrease with different slopes as a function of the distance (ca. d^{-6}, d^{-10} and d^{-1}, respectively). Specific and anisotropic interactions to and from the environment are especially important for macromolecules e.g. for metalloproteins.

3.3. Modeling of properties

3.3.1. Strain energies

The classical application of empirical force field calculations is that of conformational analyses and the computation of isomer distributions [48,100,110–119]. The early work involved nearly exclusively cobalt(III) hexaamine chemistry [48,96–98,100,110–119]. The cobalt(III) amine force field has been extensively tested and found to be very reliable[3] [8]. Note, that a structural force field (minima on potential energy surfaces) does not necessarily lead to accurate predictions of strain energy differences (steepness of the potentials) [8,66]. The observation that, with some of the force fields, the predicted thermodynamic properties are in good agreement with experimental data is based on the fact that the corresponding parameter sets for the organic backbones have been fitted to thermodynamic data [8,66]. Thus, it is not unexpected that with these parameterizations isomer ratios and conformational equilibria of titanium(IV), chromium(III), iron(II), iron(III), cobalt(II), nickel(II) and copper(I) compounds are also generally in good agreement with experimental data [23,24,75,81,120,121].

---

[2] The parameters used in these functions, i.e. the moments of inertia and vibrational frequencies, together with more general parameters, are available from molecular mechanics calculations, specifically when second derivative methods are used for the minimization procedure.

[3] A recent study based on a hexaamine cobalt(III) cage compound with extremely long bonds (see Table 6) lead to the conclusion that the harmonic potentials usually used need to be replaced with a Morse function with an identical force constant and an identical ideal bond distance [81].

Table 5
Electronic parameters used in MM-AOM calculations [52–55]

Parameter (cm^{-1})	Cr(III)	*ls* Fe(III)	*ls* Fe(II)	Co(III)	Ni(II)	Cu(II)[d]
F_2[a]	1211	786	1112	1046	1243	—
F_4[a]	101	57	90	85	79	—
$e_\sigma(NH_3)$[b,c]	7200	—	—	7245	3582	—
$e_\sigma(RNH_2)$[b,c]	7400	7500	7188	7433	3857	6400
$e_\sigma(R_2NH)$[b,c]	8000	7500	7344	7715	4133	6700
$e_\sigma(R_3N)$[b,c]	8700	—	—	8186	4592	7100
e_σ(pyridine)[b,c]	—	7900	—	—	—	—
e_π(pyridine)[b,c]	—	−500	—	—	—	—
$e_\sigma(OH_2)$[c]	—	—	—	—	—	1090

[a] Condon–Shortley interelectronic repulsion parameters.

[b] For low spin iron(III) a single e_σ for the various amines was used.

[c] Normalized for Cr^{III}–N = 2.080, Fe^{III}–N = 1.985, Fe^{III}–N_{py} = 1.968, Fe^{II}–N = 2.000, Co^{III}–N = 1.980, Ni^{II}–N = 2.130, Cu^{II}–N = 2.027, Cu^{II}–O = 2.440 Å; these values are adjusted with $1/r^6$ (r = metal donor distance).

[d] $k = 0.7$, $\xi = -580$, $K = 0.43$, $P = 0.0036\ cm^{-1}$, $\alpha^2 = 0.74$.

Reduction potentials are related to the free energy of the corresponding electron transfer process. For cobalt(III/II) hexaamines and copper(II/I) tetraamines there are linear correlations between the strain energy differences ΔU_{strain} of the oxidized and reduced forms and the reduction potentials ($E° = (-a/nF)\Delta U_{strain} + b$) [31,57]. The deviation of the parameter values of a and b from the theoretically expected values of 1.0 and 0.0, respectively, is due to the neglect of solvation and entropic terms. The fact that a linear dependence of $E°$ from ΔU_{strain} is observed indicates that the neglected terms are correlated to the strain energy differences; the relatively small deviations of the slopes and intercepts from the theoretically expected values for the copper(II/I) and the cobalt(III/II) couples means that, as expected for these couples, the steric factors are predominant [31,56,57].

Both, MM-isomer and MM-redox have been used successfully for the design of new compounds with desirable properties [23,24,31,57] and for the determination of structures in solution [56,72,75,81,120].

3.3.2. Ligand field properties

Term energies of transition metal ions depend on the metal center, the donor atoms and the geometry of the coordination polyhedron. The AOM is a simplified MO treatment of the metal d-orbitals and their interaction with the donor orbitals [122–125]. The destabilization of the d-orbitals is proportional to a two-atom overlap integral, and this is parameterized with e_σ, e_π and e_δ values. The computation of spectroscopic properties, based on a combination of force field and ligand field calculations (MM-AOM) has been used successfully for the design of new compounds and for solution structure determinations [52–56,72,75]. The fact that a constant parameter set is used (see Table 5) indicates that errors due to the non-transferability of ligand field parameters [52–55,126–128] do not lead to unacceptable inaccuracies. The prediction of d–d spectra with similar concepts has recently been reviewed [129].

3.3.3. Spectra simulations

Parameters from magnetic resonance experiments are directly dependent on the relative orientation of electron and nuclear spins. Experimental spectroscopic information has been used extensively for the constraints of internal coordinates in structure optimizations. Powerful NMR techniques have been developed for the structural analysis of proteins [130,131]. More recently, methods have been developed for structural studies of macromolecules with paramagnetic metal centers [132,133]. EPR spectra of weakly dipole–dipole coupled dicopper(II) compounds have also been used to derive structural information [77–80].

4. Cobalt hexaamines

Cobalt(III)–amine bonds are, due to the low spin d^6 electronic configuration of the metal center, relatively strong, short and rigid. That is, hexaamine cobalt(III) compounds are stable and inert, the ligand fields are comparably strong, reduction potentials are rather low and deviations from octahedral coordination geometries and from averaged Co–N distances of ca. 1.97 Å are comparably small (see also Table 1 and the corresponding discussion; the reduced form has high spin d^7 electronic configuration, and these compounds are comparably labile, less rigid and have weaker ligand fields). In spite of the rigidity of cobalt(III), there are examples where carefully designed stresses in the organic backbones of the amine ligands induce deformations of the coordination geometries that lead to a wide variety of properties: colors vary from yellow to blue (difference of approximately 4000 cm^{-1} in energy of the first dd transition), reduction potentials span the range of ca. 1.5 V and electron self-exchange rates vary over ten orders of magnitude. Structural data of a range of cobalt hexaamines, including compounds with extreme structural, spectroscopic and electrochemical properties, are assembled in Table 6; the corresponding ligand structures are given in Chart 2; structural parameters are defined in Chart 3; some selected structures are presented in Fig. 3 (various review articles report more comprehensive data sets [134–136]).

Spectroscopic and electrochemical properties of the cobalt hexaamines listed in Table 6 are given in Table 7. The ligand field strength (cf. the first dd-transition energy of the cobalt(III) hexaamines given in Table 7) is, with a constant chromophore ($Co^{III}N_6$), dominated by the metal–donor distance (this also emerges from a qualitative correlation of the first column each of Tables 6 and 7; the compounds are tabulated in the order of increasing Co^{III}–N distances). Further structural parameters of importance are the nucleophilicity of the donor atom (see also Table 3), angular distortions of the chromophore (columns 2–5 in Table 6) and the direction of the donor orbitals with respect to the metal–donor vector (misdirected valences, see last column in Table 6). All these factors are included in AOM calculations, and ligand field spectroscopic properties, computed by the MM-AOM approach, have been shown to be rather accurate. This is also demonstrated in Table 7.

A ligand that enforces small metal–donor distances will stabilize the oxidized form (comparably low, negative reduction potential, e.g. [Co(*trans*-diammac)]$^{3+/2+}$ in Table 7); a ligand with a relatively large cavity will stabilize the reduced metal ion (comparably high, positive reduction potential, e.g. *lel*$_3$-[Co(src)]$^{3+/2+}$ in Table

Table 6
Structural parameters of some cobalt hexaamines[a]

	Co–N (Å)	α[b]	γ	θ	∅	Co–N–C (°)	Refs.
Co(*trans*-diammac)[c]	1.946, 1.937	—	—	9	—	106	[43]
	2.125, 2.088	—	—	8	—	104	[38,44–46,99–101]
$Co(NH_3)_6$	1.960	90	180	0	60	—	[137]
	2.170	90	180	0	60	—	[134]
$Co(en)_3$[d]	1.964	86	175	—	55	108	[138,139]
	1.990	86	174	—	52	108	[38,44–46,99–101]
Co(sar)[e]	1.974	87	—	—	57	112	[140,141]
	2.151	82	—	—	33	112	[38,44–46]
$Co(tn)_3$	1.983	88	177	—	55	119	[142]
	2.166	85	172	—	51	115	[38,44–46]
ob$_3$-Co(src)	1.990	90	—	—	60	116, 120	[143]
	2.124	92	—	—	61	112,116	[81]
$Co(tmen)_3$[f]	1.997	80	167	—	44	116	[136,144]
	2.193	75	159	—	26	113	[136,144]
lel$_3$-Co(src)	2.046	89	—	—	59	115	[81]
	2.235	88	—	—	43	111,118	[143]

[a] For ligand abbreviations see Chart 2; for structural parameters see Chart 3; first line: cobalt(III), second line cobalt(II).

[b] Bite angle of the smallest chelate ring.

[c] Co(III): $\lambda\delta$-conformer; Co(II): $\delta\delta$-conformer; bond distances: axial, equatorial.

[d] Co(III): *lel*$_3$; Co(II): *lel*$_3$.

[e] Co(III): D_3*lel*$_3$; Co(II): D_3*lel*$_3$.

[f] ob_3 conformations.

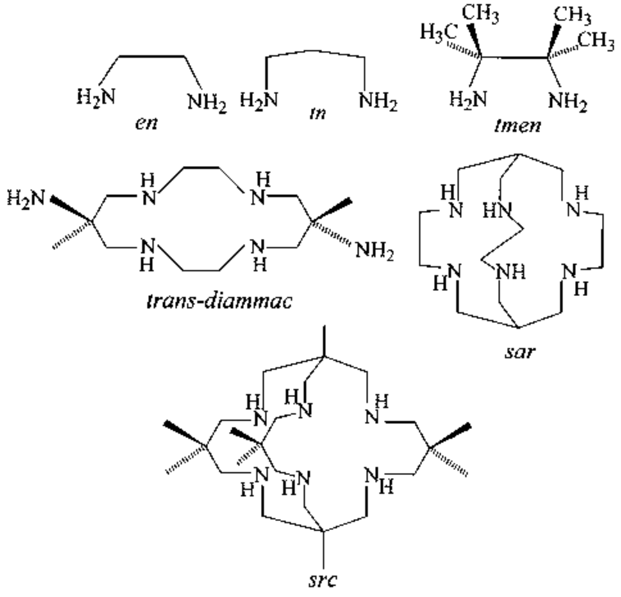

Chart 2.

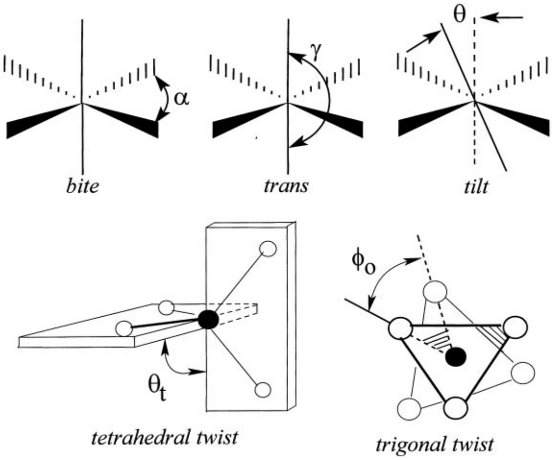

Chart 3.

7). It follows that the ligand field properties and reduction potentials may be correlated. There has been a lively discussion on this subject [134,135,145–149]. The important points here are:

1. There are steric contributions to both the reduction potentials and the ligand

Table 7
Molecular properties of some cobalt hexaamines[a]

	ν_1[b] ($\mathrm{cm^{-1}}$)	$E°$[c] (V)	k_{self}[d] ($\mathrm{M^{-1}\,s^{-1}}$)
Co(*trans*-diammac)	22170	-0.63	6.8×10^{2}
	23090	*-0.79*	*1.7×10^{1}*
Co(NH_3)$_6$	21050	-0.02	1×10^{-6}
	21180	*-0.10*	*3.5×10^{-5}*
Co(en)$_3$	21370	-0.17	2.9×10^{-5}
	21190	*-0.15*	*2.3×10^{-4}*
Co(sar)	21230	-0.40	2.1×10^{-0}
	21240	*-0.41*	*7.7×10^{-1}*
Co(tn)$_3$	20600	$+0.13$	—
	20590	*$+0.16$*	—
ob$_3$-Co(src)	20833	0.0	—
	20790	*-0.10*	—
Co(tmen)$_3$	19841	$+0.28$	8.5×10^{-8}
	—	*$+0.32$*	*8.5×10^{-8}*
lel$_3$-Co(src)	16667	$+0.84$	—
	16340	*$+0.89$*	—

[a] First line: experimentally determined, second line: calculated (italics).

[b] Low energy d–d transition of cobalt(III) [$^1A_{1g}\rightarrow{}^1T_{1g}$ (O_h)] [31,52–54,81,143,144].

[c] Reduction potential versus SHE [31,81,143,144].

[d] Electron self-exchange rate [31,144].

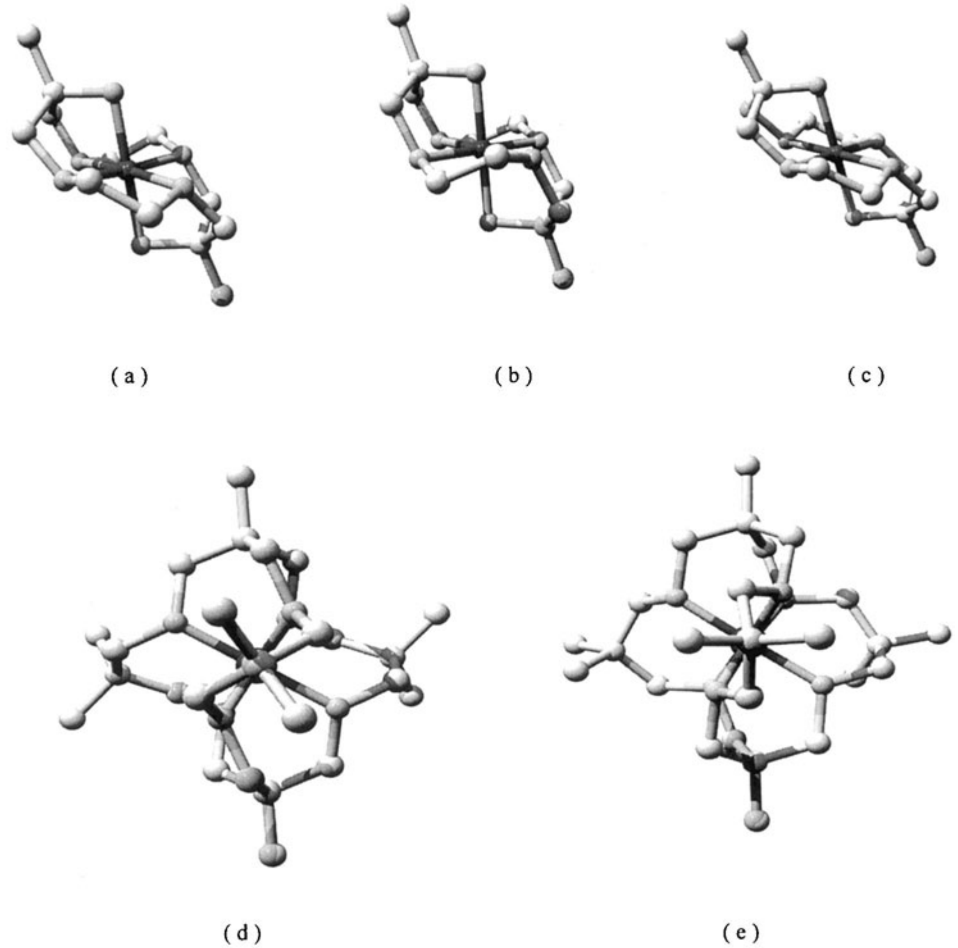

Fig. 3. Computed structures of the three isomers of $[Co(\textit{trans}\text{-diammac})]^{3+}$ (a: $\delta\delta$, b: $\lambda\delta$, c: $\delta\lambda$) and of the two isomers of $[Co(src)]^{3+}$ (d: ob_3, e: lel_3); hydrogen atoms are omitted for clarity; for the structure of the ligands, see Chart 2.

field strengths, and the expectation is that, therefore, these parameters are correlated

2. The reduction potential is related to the energy difference between the ground states of the oxidized and the reduced form; the ligand field strength depends on the energies of the ground state and the excited state of a given oxidation state; thus, there is not necessarily a simple correlation between the two properties
3. For reduction potentials (and ligand field spectroscopic properties) steric effects are just one of the important factors. Others include electronic effects (i.e. the type, symmetry and relative orientation of the donor and acceptor orbitals), interactions with the environment and entropic factors.

Simple correlations such as those leading to the computed reduction potentials in Table 7 (see also Section 3.3) are based on data sets with a constant metal center and a common type of donor; differentiation between ammonia, primary, secondary and tertiary amines increases, as expected, the accuracy (see Table 3) [31,57]. The rationale for MM-redox, i.e. the computation of reduction potentials based on steric strain, is simple thermodynamics (Eqs. (1) and (2))

$$\Delta G^\circ = -nFE^\circ \tag{1}$$

$$\Delta G^\circ = I + \Delta(\Delta G^\circ_c) + \Delta(\Delta G^\circ_{aq}) \tag{2}$$

where F is the Faraday constant, I is the ionization potential, ΔG°_c is the complexation free energy of the oxidized and reduced forms in the gas phase and ΔG°_{aq} is the corresponding solvation free energy. Some other concepts for the computation of reduction potentials have been reviewed [150]. A rather successful approach uses general electrochemical parameters [151–155]. In contrast to MM-redox this is based on metal–donor bonding and neglects steric effects. It is obvious that the two approaches have limited and different areas of applicability [31].

Force field calculations [31,156] and similar approaches [157] have been used also to compute electron self exchange rates. Some of the results emerging from molecular mechanics are also shown in Table 7. It appears that the predicted order of magnitude is correct but the overall accuracy is inferior to that of the predicted reduction potentials and electronic spectroscopic properties. The computed self-exchange rates are based on a first-order harmonic model (see Fig. 4): the difference in energy between the crossing point of two potential energy curves and that of the corresponding minima is correlated with the electron self-exchange rate [$k_{\mathrm{self}} = f(\Delta G^{\neq})$; $\Delta G^{\neq} \sim \Delta U^{\neq}_{\mathrm{strain}}$; $\Delta U^{\neq}_{\mathrm{strain}} = 2\Delta U_{\mathrm{strain}}$ (cross) $- \Delta U_{\mathrm{strain}}$ ($\mathrm{Co^{III}}$) $- \Delta U_{\mathrm{strain}}$ ($\mathrm{Co^{II}}$)]. Apart from the approximations discussed above (neglecting intermolecular interactions, specific electronic terms and entropic strain), there is the additional problem of finding the structure where both reactants (cobalt(III) and cobalt(II) forms) have the same nuclear configuration and where the sum of the distortion energies is at a minimum [31]. The problem is that this does not necessarily mean

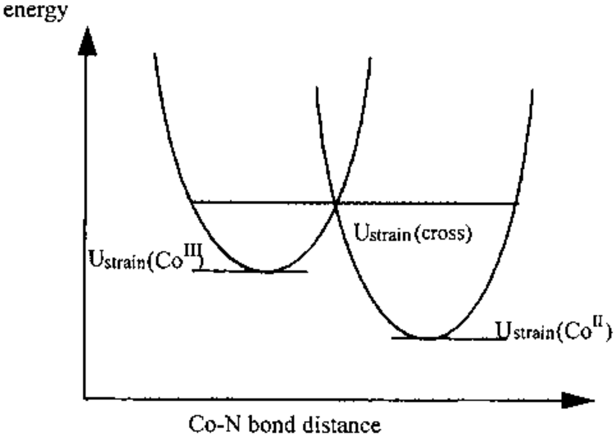

Fig. 4. Visualization of the activation free energy for an electron self-exchange process.

that the strain energies of the activated reduced and oxidized forms are identical, i.e. the situation shown in Fig. 4 corresponds to a simplification. This and the expected and observed inaccuracies have been discussed in detail [31].

Recent work on cobalt(III) hexaamine cage complexes indicates that well designed but relatively small structural changes on hexaamine cage ligands may lead to stresses that have profound effects in terms of the spectroscopic and electrochemical properties (see Tables 6 and 7) [81,143]. *Trans*-diammac is a ligand that, due to a very tight fit, based on five-membered chelate rings involving the primary amine donor groups, leads generally to extremely strong ligand fields [52]. The corresponding *cis*-derivative is much less spectacular in this respect [158]. However, a cage ligand based on *cis*-diammac, where the two primary amine donors are linked with an ethyl group, might produce a very rigid and high ligand field hexaamine cage ligand molecule. This hexaamine is a derivative of 'sar' with two methylene groups abstracted ('diabsar'); the corresponding 'absar' ligand with only one of the two methylene groups abstracted has been reported [159]. The calculated structures of the cobalt(III) compound of the two isomers of diabsar (see Chart 4) are shown in Fig. 5 (note that *s*-diabsar is the derivative of *cis*-diammac; note also that the methyl substituents of

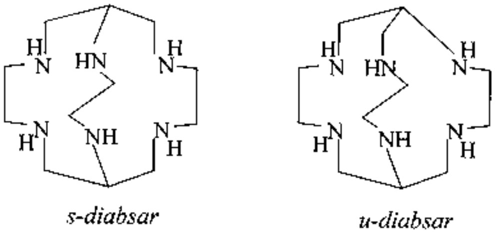

Chart 4.

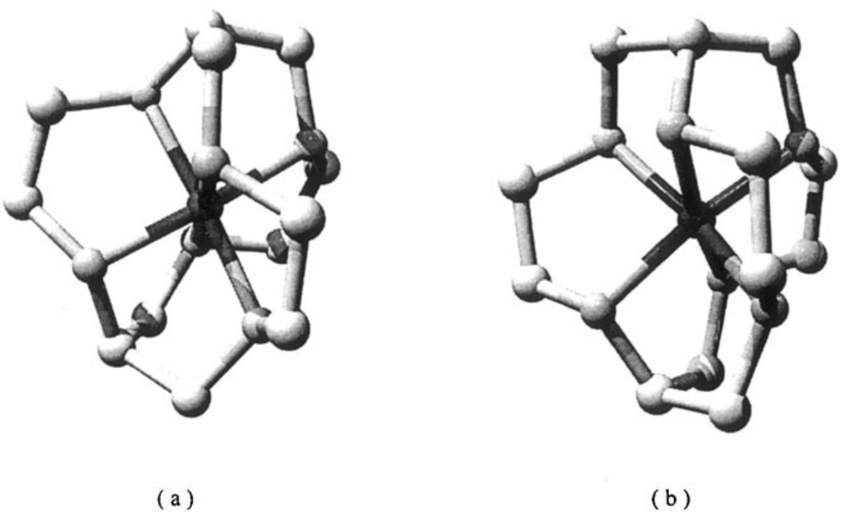

Fig. 5. Strain energy minimized structures of (a) [Co(*s*-diabsar)]$^{3+}$ and (b) [Co(*u*-diabsar)]$^{3+}$; methyl groups at the two apical carbon atoms and hydrogen atoms omitted.

cis-diammac, leading to quaternary carbon atoms, are omitted in Chart 4 and Fig. 5).

Based on the structure shown in Fig. 5 and with the methods and parameter sets used for the computation of the ligand field electronic spectra (MM-AOM) and reduction potentials (MM-redox) for the hexaamine cobalt(III/II) couples in Tables 6 and 7, the corresponding properties of $[\mathrm{Co(diabsar)}]^{3+/2+}$ have been computed. Only the most stable conformer (*lel₃*) of one of the isomers (*s*-diabsar in Chart 4 and Fig. 5, i.e. that based on $[\mathrm{Co}(cis\text{-diammac})]^{3+}$) has been considered in this preliminary study. Note, that the shortest $\mathrm{Co^{III}{-}N}$ distances computed for this compound ($\mathrm{Co{-}N} = 1.936$ Å) are at the shorter end of $\mathrm{Co^{III}{-}N}$ distances used for the parameterization of our force field. Since molecular modeling is based on interpolations [8], the predictions for $[\mathrm{Co}(s\text{-diabsar})]^{3+}$ must be treated with some caution. The computed reduction potential of $[\mathrm{Co}(s\text{-diabsar})]^{3+}$ ($E° = -0.61$ V) is, as expected, similar to that of $[\mathrm{Co}(trans\text{-diammac})]^{3+}$ and the computed first ligand field transition ($^1A_1 \rightarrow {}^1T_1$) at 24 800 $\mathrm{cm^{-1}}$ (405 nm) indicates that the ligand field may indeed be extremely strong.

5. Iron hexaamines

The nitrogen donor coordination chemistry of iron(II) and (III) is dominated by π-donor and -acceptor ligands, i.e. by porphyrines and pyridine derivatives such as bipy (2,2′-bipyridine), phen (1,10-phenanthroline) and terpy (2,2′:6′,2″-terpyridine), respectively. Iron(II) compounds with mixed aliphatic/aromatic amine coordination spheres often have interesting electronic properties, since they are close to the spin crossover point, and there is an extensive literature on spin equilibria in iron(II) compounds [160–162]. Light-induced spin state conversion has been observed in some systems, and this opens the possibility for the construction of advanced optical materials, including materials for optical data storage. The interesting ligand field spectroscopic properties of spin-equilibrium (and low spin) iron(II) compounds are usually obscured by intense charge transfer transitions at relatively low energy. Only a limited number of hexaamine iron(II) systems with aliphatic ligands are known that are stable enough to be studied spectroscopically and structurally in solution and in the solid state.

Low spin iron(III) compounds have been of interest to probe the Jahn–Teller instability of the $^2T_{2g}$ ground state (in O_h symmetry) and, due to the large variation of g-values as a function of the splitting of the ground state, EPR spectroscopy is a very useful technique to probe the coordination geometry. However, the ground state splitting is very sensitive to π-bonding and, therefore, amine ligand systems are required to probe the influence of geometric distortions due to Jahn–Teller effects alone. Also, until recently, the interpretation of the EPR spectra of low spin iron(III) hexaamines, based on ligand field theory, was less than satisfactory [74]. Due to the importance of low spin iron(III) (and iron in general) in biological systems, a thorough understanding of the corresponding electronic and spectroscopic properties is needed.

Table 8
Experimental data for $Fe^{II/III}(tacn)_2$, $Fe^{II/III}$(*trans*-diammac) and $Fe^{II/III}$(diamsar)

	$Fe(tacn)_2$	Fe(diamsar)	Fe(*trans*-diammac)
Refs.	[163–165]	[166,167]	[53,74,75,168]
Ground state Fe^{II}	$^1A_1$ ($^5T_2$)	($^1A_1$) $^5T_2$	$^1A_1$
Ground state Fe^{III}	$^2T_2$	$^2T_2$	$^2T_2$
$E°$ ($Fe^{III/II}$) (V)	0.13	0.65	0.45
Fe^{II}–N (Å)	2.03	2.21	2.007, 2.030
Fe^{III}–N (Å)	1.99	2.007	1.968, 1.984
$\varnothing, \theta^{a}$ (Fe^{II}) (°)	59	28.6	11.5
$\varnothing, \theta^{a}$ (Fe^{III}) (°)	58	53	10.5
ν_1, ν_2 (Fe^{II}) (cm^{-1})	16639, 25840	16949, 25381	17123, 24691
g_1, g_2, g_3 (Fe^{III})	—	—	1.63, 2.46, 2.84

[a] See Chart 2 for definition of the structural parameters.

There are only very few hexaamine systems, where full experimental details on the iron(II) and (III) forms have been reported. These include *trans*-diammac, diamsar (see Chart 1; diamsar is the bis NH_2-derivative of sar, i.e. the apical tertiary carbon atoms (caps) are amine-substituted) and tacn (see Chart 5). Experimental data for the iron(II) and (III) compounds of these ligands are given in Table 8.

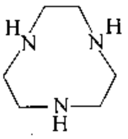

tacn

Chart 5.

From Table 8, it emerges that for both iron(II) and (III), *trans*-diammac leads to the shortest Fe–N distances in the series and, therefore, to the highest ligand field. For iron(II), there is no indication for any contribution of the high spin electronic configuration, even at elevated temperatures (up to 325 K, solid state and aqueous solution) [75].

Results of MM-AOM calculations of the three low spin iron(II) compounds and of the low spin iron(III) form of the *trans*-diammac compound are given in Table 9. The good agreement between observed and computed spectroscopic properties for these compounds (and for others reported in the literature [53,74,75]) allows an accurate structural assignment of the *trans*-diammac complexes. For iron(II) and (III) the compounds observed in solution and in the solid state have, according to the MM-AOM analysis, $\delta\delta$ conformation. While, for iron(II), this was obvious already from the X-ray crystal structural analysis

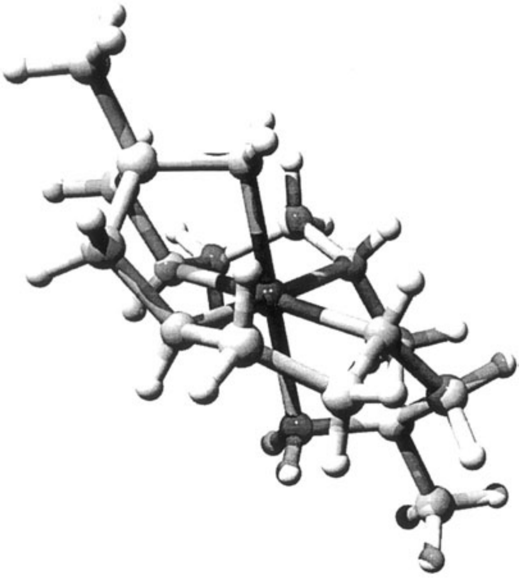

Fig. 6. Plot of the molecular cation of [Fe(*trans*-diammac)](PF_6)$_2$, obtained by X-ray diffraction.

(see Fig. 6) [75], that of the iron(III) complex was disordered [74,168]. Here, the MM-AOM analysis was used to determine the conformation of this compound in the solid and in solution [53].

Table 9
Calculated (MM-AOM) and observed electronic transitions of low-spin iron(II) hexaamine complexes

	Strain energy (kJ mol^{-1})	ν (cm^{-1}) (g_1, g_2, g_3)		Refs.
[Fe(*trans*-diammac)]$^{2+}$				
$\delta\delta$ (MM-AOM)	82.2	17400	25900	[75]
$\delta\lambda$ (MM-AOM)	96.5	15500	23100	
$\lambda\delta$ (MM-AOM)	87.4	18900	27600	
Observed ($\delta\delta$)		17100	24700	[75]
[Fe(*trans*-diammac)]$^{3+}$				
$\delta\delta$ (MM-AOM)	91	1.45, 2.54, 2.95		[53]
$\delta\lambda$ (MM-AOM)	112	1.89, 2.05, 2.46		
$\lambda\delta$ (MM-AOM)	92	0.95, 1.96, 3.29		
Observed		1.5, 2.6, 2.8		[53,74,168]
[Fe(tacn)$_2$]$^{2+}$				
(MM-AOM)		16600	24900	[75]
Observed		16600	25800	[163–165]
[Fe((NH$_2$)$_2$sar)]$^{2+}$				
(MM-AOM)		16400	24700	[75]
Observed		16900	25400	[166,167]

6. Copper tetraamines

The correlation of structural, spectroscopic and redox properties has a long tradition in the area of copper(II) chemistry. This is partly due to the biological importance of copper compounds and interesting properties of copper proteins, but also to the broad range of coordination geometries which are available in classical copper coordination compounds. Correlations of interest that have been reported include those of $g_{||}$ and $A_{||}$ values (Blumberg-Peisach plots) [169], the inverse correlation between equatorial and axial bonds in tetragonal copper(II) complexes [170,171] and various correlations that include resonance Raman, electronic spectroscopic and structural parameters of copper proteins [172–175].

Copper(II) tetraamines usually have $4+1$ or $4+2$ chromophores with the four amine donors in a distorted planar arrangement and one or two more distant axial donors (solvent molecules, side chains of a multidentate ligand or anions) completing the coordination sphere. With tetraazamacrocyclic ligands the distortion of the in-plane field is controlled by the size (and geometry) of the macrocyclic ring, and 14-membered macrocycles of the type of cyclam (1,4,8,11-tetraazacyclotetradecane; $a = c = (CH_2)_2$, $b = (CH_2)_3$ in Chart 6) are most suitable for copper(II). Smaller macrocycles usually lead to five-coordinate square pyramidal geometries, with the copper(II) center above the plane of the macrocyclic ligand donors, and larger macrocycles accommodate the ca. 2.0 Å Cu–N distances through a tetrahedral twist. An example with four tetraazamacrocyclic ligands (13- to 16-membered, see Chart 6) is presented in Figs. 7 and 8 and Table 10: Fig. 7 visualizes the distortion of the chromophore as a function of the macrocycle ring size. The plots in Fig. 8 indicate that the spectroscopic and electrochemical properties all follow the same pattern.

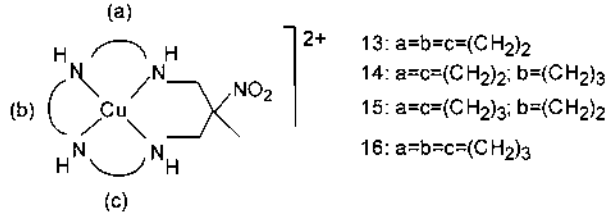

Chart 6.

From the data presented in Table 10, it emerges that, as expected from other studies, there is excellent agreement between computed and observed structural, spectroscopic (MM-AOM) and electrochemical (MM-redox) data. Also of interest is the observation, emerging from Fig. 8, that the relevant molecular properties of the four CuN_4 compounds (reduction potentials, electronic and EPR spectra) are strongly correlated to the coordination geometry, represented by the twist angle θ that describes the geometry of the central CuN_4 chromophore (see Chart 3). Thus,

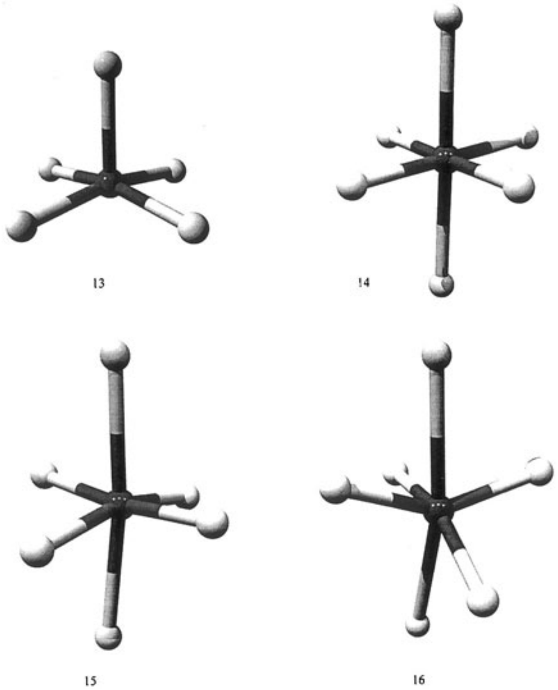

Fig. 7. Calculated structures of the chromophores of $[Cu([13]N_4)](OH_2)$, $[Cu([14]N_4)](OH_2)_2$, $[Cu([15]N_4)](O)(OH_2)$ and $[Cu([16]N_4)](O)(OH_2)$; the first oxygen donor in the two latter structures is from the pendent nitro group of the macrocyclic ligand [54].

the computation of spectroscopic and electrochemical properties of copper (II) tetraamines may be based on correlation functions obtained from the compounds discussed here, i.e. on pattern search and interpolation, and this is a general basis for molecular modeling [56]. It may appear that interpretations based on simple correlations, such as those emerging from Fig. 8, are less rigorous than discussions based on well established computations as, for example, those leading to the data presented in Table 10 (see, however, discussions on ‘model and reality’ in recent articles [56,66]; note also, that from Fig. 8 it appears that the reduction potentials $E°$ are correlated to the ligand field strengths ν_1; the lack of a theoretical basis for such a correlation has been discussed above in Section 4 [134,135,145–149]). However, recent observations in the area of blue copper proteins that involve structural, spectroscopic and electron transfer properties of wild-type and mutated species, indicate that the correlation of structural deformations with electronic properties may help to predict the behavior of new mutants and determine structures in solution, and to further the understanding of fundamental principles in this area [172–175].

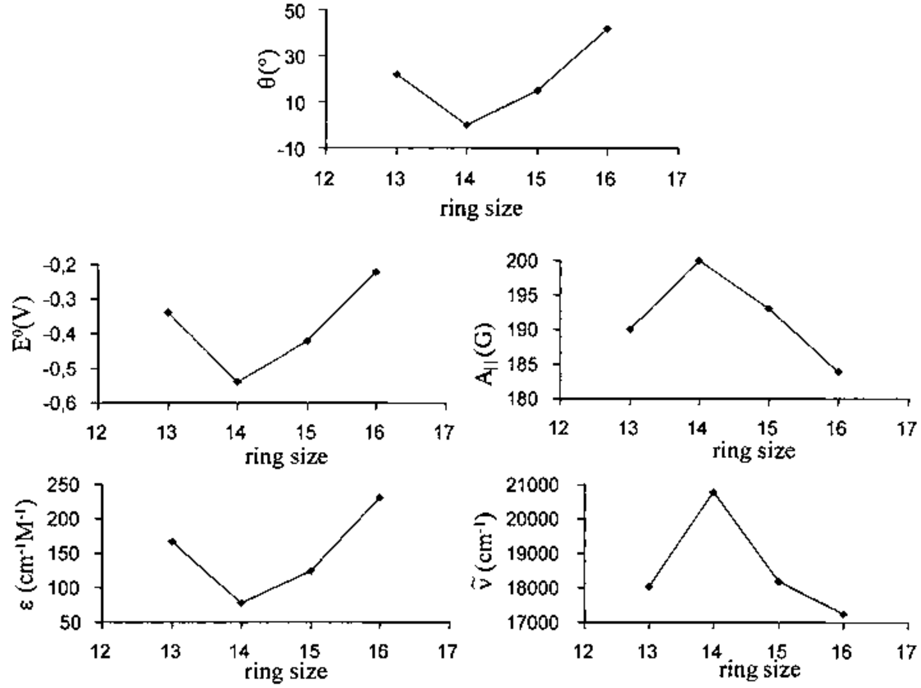

Fig. 8. Correlation of the CuN_4 plane twist angle θ (see Chart 3), the reduction potential $E°$, the EPR hyperfine parameter $A_{||}$, the d–d transition ν_1 and its extinction coefficient ε_1 with the macrocycle ring size [54,57,176].

Table 10
Experimentally determined and calculated (italics) structural and spectroscopic parameters (MM-AOM in brackets) of a series of copper(II) tetraamines [54,57,176]

Compound[a]	Cu–N$_{av}$ (Å)	Cu–X$_{av}$ (Å)		θ_{av} (°)[b]	E_{xy} (cm^{-1})	$E°$ (mV)
$[Cu([13]N_4)]^{2+}$	2.014	1	(2.507)[c]	28.0	18020 (*19530*)	−0.34
	1.999		*2.195*	*21.6*	*18640*	*−0.41*
$[Cu([14]N_4)]^{2+}$	2.006	2	2.558	0.3	20830 (*21200*)	−0.54
	2.019		*2.549*	*1.1*	*20400*	*−0.51*
$[Cu([15]N_4)]^{2+}$	2.037	2	2.512	11.5	18180 (*18840*)	−0.42
	2.038		*2.493*	*17.2*	*18340*	*−0.40*
$[Cu([16]N_4)]^{2+}$	2.029	2	2.643	35.3	17240 (*18080*)	−0.22
	2.008		*2.682*	*42.5*	*17850*	*−0.18*

Acknowledgements

These studies are supported by the German Science Foundation (DFG), the Fonds of the Chemical Industry (FCI) and the VW-Stiftung. I am grateful for this support and, indeed, for the excellent work done by all my coworkers whose names appear in the references. I would also like to thank Karin Stelzer for her help in preparing the manuscript.

References

[1] D.J. Cram, T. Kamda, R.L. Helgeson, G.M. Liu, J. Am. Chem. Soc. 99 (1979) 948.
[2] D.J. Cram, G.M. Liu, J. Am. Chem. Soc. 107 (1985) 3657.
[3] P. Comba, A. Fath, A. Kühner, B. Nuber, J. Chem. Soc. Dalton Trans. (1997) 1889.
[4] R.D. Hancock, Progr. Inorg. Chem. 37 (1989) 187.
[5] R.D. Hancock, in: A.F. Williams, C. Floriani, A.E. Berbach (Eds.), Perspectives in Coordination Chemistry, VCH, Weinheim, 1992, p. 129.
[6] R.D. Hancock, Acc. Chem. Res. 23 (1990) 253.
[7] D.H. Busch, Acc. Chem. Res. 11 (1978) 392.
[8] P. Comba, T.W. Hambley, Molecular Modeling of Inorganic Compounds, VCH, Weinheim, 1995.
[9] P. Comba, K. Gloe, T. Inoue, H. Stephan, K. Yoshizuka, Inorg. Chem. 37 (1998) 3310.
[10] B.P. Hay, D. Zhang, J.R. Rustad, Inorg. Chem. 35 (1996) 2650.
[11] B.P. Hay, J.R. Rustad, C.J. Hostetler, J. Am. Chem. Soc. 115 (1993) 11158.
[12] B.P. Hay, J.R. Rustad, Supramol. Chem. 6 (1996) 383.
[13] B.P. Hay, J.R. Rustad, J. Am. Chem. Soc. 116 (1994) 6316.
[14] P. Comba, Coord. Chem. Rev. (1998) submitted for publication.
[15] E. Fischer, Chem. Ber 27 (1894) 2985.
[16] K.B. Lipkowitz, J. Chromatogr. A 666 (1994) 493.
[17] K.B. Lipkowitz, J. Chromatogr. A 694 (1995) 15.
[18] K. Miyoshi, S. Izumoto, K. Nakai, H. Yoneda, Inorg. Chem. 25 (1986) 4654.
[19] H. Nakazawa, U. Sakaguchi, H. Yoneda, J. Am. Chem. Soc. 104 (1982) 3885.
[20] T. Taura, J. Am. Chem. Soc. 101 (1979) 4221.
[21] K. Bernauer, Top. Curr. Chem. (Springer) 65 (1976) 1.
[22] V.A. Davankov, in: V.A. Davankov, J.D. Navratil, H.F. Walton (Eds.), Ligand Exchange Chromatography, CRC Press, Boca Raton, FL, 1988.
[23] P.V. Bernhardt, P. Comba, T.W. Hambley, I. Sóvágó, K. Várnagy, J. Chem. Soc. Dalton Trans. (1993) 2023.
[24] P.V. Bernhardt, P. Comba, T. Gyr, K. Várnagy, Inorg. Chem. 31 (1992) 1220.
[25] C.G. Frost, J. Howarth, J.M.J. Williams, Tetrahedron Asymmetry 3 (1992) 1089.
[26] B.M. Trost, D.L. van Vranken, Chem. Rev. 96 (1996) 395.
[27] P.-O. Norrby, B. Akermark, F. Haeffner, S. Hansson, M. Blomberg, J. Am. Chem. Soc. 115 (1993) 4859.
[28] M.M. Gugelchuk, K.N. Houk, J. Am. Chem. Soc. 116 (1994) 330.
[29] R.J. Deeth, I.J. Munslow, V.J. Paget, in: L. Banci, P. Comba (Eds.), Molecular Modeling and Dynamics of Bioinorganic Systems, Kluwer, Dordrecht, 1997, p. 77.
[30] C.R. Landis, T.K. Firman, T. Cleveland, D.M. Root, in: L. Banci, P. Comba Jr. (Eds.), Molecular Modeling and Dynamics of Bioinorganic Systems, Kluwer, Dordrecht, 1997, p. 49.
[31] P. Comba, A.F. Sickmüller, Inorg. Chem. 36 (1997) 4500.
[32] P. Comba, A. Kühner (1998) submitted for publication.
[33] R. Lumry, H. Eyring, J. Phys. Chem. 58 (1954) 110.
[34] B.L. Vallee, R.J.P. Williams, Proc. Natl. Acad. Sci. USA 59 (1968) 498.
[35] J.A. Yankeelov Jr., D.E. Koshland, J. Biol. Chem. 240 (1965) 1593.
[36] W.W. Cleland, Acc. Chem. Res. 8 (1975) 145.
[37] A.G. Orpen, L. Brammer, F.H. Allen, O. Kennard, D.G. Watson, R. Taylor, J. Chem. Soc. Dalton Trans. (1989) S1.
[38] P. Comba, T.W. Hambley, N. Okon, G. Lauer, MOMEC—a molecular modeling package for inorganic compounds, CVS, Heidelberg, 1997, e-mail:cvs@t-online.de.
[39] H. Yoneda (1998) unpublished results.

[40] P. Comba, Coord. Chem. Rev. 123 (1993) 1.
[41] R.D. Hancock, A.E. Martell, Chem. Rev. 89 (1989) 1875.
[42] R.D. Hancock, A.E. Martell, Comments Inorg. Chem. 6 (1988) 237.
[43] P.V. Bernhardt, G.A. Lawrance, T.W. Hambley, J. Chem. Soc. Dalton Trans. (1989) 1059.
[44] P.V. Bernhardt, P. Comba, Inorg. Chem. 31 (1992) 2638.
[45] P. Comba, T.W. Hambley, M. Ströhle, Helv. Chim. Acta. 78 (1995) 2042.
[46] J.E. Bol, C. Buning, P. Comba, J. Reedijk, M. Ströhle, J. Comput. Chem. 19 (1998) 512.
[47] P. Comba, T.W. Hambley, in: T. Clark (Ed.), Molecular Mechanics of Inorganic Compounds, Hypercube, Gainsville, FL, 1998.
[48] M.R. Snow, J. Am. Chem. Soc. 92 (1970) 3610.
[49] G.R. Brubaker, D.W. Johnson, Inorg. Chem. 22 (1983) 1422.
[50] G. Golub, H. Cohen, P. Paoletti, A. Bencini, L. Messori, I. Bertini, D. Meyerstein, J. Am. Chem. Soc. 117 (1995) 8353.
[51] P.V. Bernhardt, J. Am. Chem. Soc. 119 (1997) 771.
[52] P.V. Bernhardt, P. Comba, Inorg. Chem. 32 (1993) 2798.
[53] P. Comba, Inorg. Chem. 33 (1994) 4577.
[54] P. Comba, T.W. Hambley, M.A. Hitchman, H. Stratemeier, Inorg. Chem. 34 (1995) 3903.
[55] P. Comba, P. Hilfenhaus, B. Nuber, Helv. Chim. Acta. 80 (1997) 1831.
[56] P. Comba, in: W. Gans, A. Amann, J.C.A. Boeyens (Eds.), Fundamental Priciples of Molecular Modeling, Plenum Press, New York, 1996, p. 167.
[57] P. Comba, H. Jakob, Helv. Chim. Acta 80 (1997) 1983.
[58] H. Irving, R.J.P. Williams, J. Chem. Soc. (1953) 3192.
[59] H. Irving, R.J.P. Williams, Nature 162 (1948) 746.
[60] C.S.G. Phillips, R.J.P. Williams, Inorganic Chemistry, Oxford University Press, Oxford, 1965.
[61] J.E. Huheey, Inorganic Chemistry—Principles of Structure and Reactivity, 2nd ed., Harper and Row, New York, 1978.
[62] M.V. Veidis, G.H. Schreiber, T.E. Gough, G.J. Palenik, J. Am. Chem. Soc. 91 (1969) 1859.
[63] R. Meier, M. Boddin, S. Mitzenheim, K. Kanamori, in: H. Sigel (Ed.), Metal Ions in Biological Systems, vol. 31, Marcel Dekker, New York, 1996, p. 45.
[64] P. Comba, in: W. Gans, J.C.A. Boeyens (Eds.), Intermolecular Interactions, Plenum Press, New York, 1998.
[65] P. Comba, in: J.K.A. Howard, F.H. Allen (Eds.), Implications of Molecular and Materials Structure for New Technologies, Kluwer, Dordrecht, 1998, Chapter 11.
[66] P. Comba, in: J.K.A. Howard, F.H. Allen (Eds.), Implications of Molecular and Materials Structure for New Technologies, Kluwer, Dordrecht, 1998, Chapter 12.
[67] P. Comba, in: L. Banci, P. Comba (Eds.), Molecular Modeling and Dynamics of Bioinorganic Systems, Kluwer, Dorderecht, 1997, p. 21.
[68] B.P. Hay, Coord. Chem. Rev. 126 (1993) 177.
[69] R. Deeth, J. Struct. Bonding (Berlin) 82 (1995) 1.
[70] C.R. Landis, D.M. Root, T. Cleveland, in: K.B. Lipkowitz, D.B. Boyd (Eds.), Molecular Mechanics Force Field for Modeling Inorganic and Organometallic Compounds, vol. 6, VCH Verlag, New York, 1995.
[71] A.K. Rappé, C.J. Casewit, Molecular Mechanics Across Chemistry, University Science, Sausalito, 1997.
[72] P. Comba, Comments Inorg. Chem. 16 (1994) 133.
[73] M. Gerloch, CAMMAG—a FORTRAN program for AOM calculations, University Press Cambridge, Cambridge.
[74] H. Stratemeier, M.A. Hitchman, P. Comba, P.V. Bernhardt, M.J. Riley, Inorg. Chem. 30 (1991) 4088.
[75] H. Börzel, P. Comba, H. Pritzkow, A. Sickmüller, Inorg. Chem. 37 (1998) 3853.
[76] T.D. Smith, J.R. Pilbrow, Coord. Chem. Rev. 13 (1974) 173.
[77] P.V. Bernhardt, P. Comba, T.W. Hambley, S.S. Massoud, S. Stebler, Inorg. Chem. 31 (1992) 2644.
[78] P. Comba, P. Hilfenhaus, J. Chem. Soc. Dalton Trans. (1995) 3269.
[79] P. Comba, T.W. Hambley, P. Hilfenhaus, D.T. Richens, J. Chem. Soc. Dalton Trans. (1996) 533.
[80] P. Comba, R. Cusack, D.P. Fairlie, L.R. Gahan, G.R. Hanson, U. Kazmaier, A. Ramlow (1998) submitted for publication.

[81] P. Comba, A.F. Sickmüller, Angew. Chem. Int. Ed. Engl. 36 (1997) 2006.
[82] R.H. Boyd, J. Chem. Phys. 49 (1968) 2574.
[83] K.B. Wiberg, R.H. Boyd, J. Am. Chem. Soc. (1972) 8426.
[84] M.W. Thomas, D. Emerson, J. Mol. Struct. 16 (1973) 473.
[85] B. van de Graaf, J.M.A. Baas, Recl. Trav. Chim. Pays-Bas 99 (1980) 327.
[86] T.W. Hambley, J. Comput. Chem. 8 (1987) 651.
[87] P. Comba, N. Okon, R. Remenyi (1998) submitted for publication.
[88] L.Y. Martin, L.J. DeHayes, L.J. Zompa, D.H. Busch, J. Am. Chem. Soc. (1974) 4046.
[89] R.D. Hancock, J. Chem. Soc. Dalton Trans. (1986) 2505.
[90] M.G.B. Drew, P.C. Yates, J. Chem. Soc. Dalton Trans. (1986) 2506.
[91] M.G.B. Drew, S. Hollis, P.C Yates, J. Chem. Soc. Dalton Trans. (1985) 1829.
[92] I.B. Bersuker, Electronic Structure and Properties of Transition Metal Compounds, Wiley, New York, 1996.
[93] F. Maseras, K. Morokuma, J. Comput. Chem. 16 (1995) 1170.
[94] A.L. Tchougréeff, in: L. Banci, P. Comba III (Eds.), Molecular Modeling and Dynamics of Bioinorganic Systems, Kluwer, Dorderecht, 1997, p. 217.
[95] P. Comba, M. Zimmer, Inorg. Chem. 33 (1994) 5368.
[96] P. Comba, T.W. Hambley, L. Zipper, Helv. Chim. Acta 71 (1988) 1875.
[97] P. Comba, M. Maeder, L. Zipper, Helv. Chim. Acta 72 (1989) 1029.
[98] P. Comba, A. Hörmann, L.L. Martin, L. Zipper, Helv. Chim. Acta 73 (1990) 874.
[99] L.J. DeHayes, D.H. Busch, Inorg. Chem. 12 (1973) 1505.
[100] J.R. Gollogly, C.J. Hawkins, J.K. Beattie, Inorg. Chem. 10 (1971) 317.
[101] C.J. Hilleary, T.F. Them, R.E. Tapscott, Inorg. Chem. 19 (1980) 102.
[102] L. Banci, P. Comba (Eds.), Modeling of Structures and Molecular Properties of Transition Metal Compounds Toward Metalloprotein Modeling, Kluwer, Dorderecht, 1997.
[103] S.R. Cox, D.E. Williams, J. Comput. Chem. 2 (1981) 304.
[104] L.E. Chirlian, M.M. Francl, J. Comput. Chem. 8 (1987) 894.
[105] R.J. Abraham, L. Griffiths, P. Loftus, J. Comput. Chem. 3 (1982) 407.
[106] A.K. Rappé, W.A. Goddard III, J. Phys. Chem. 95 (1991) 3358.
[107] J. Sabolovic, K. Rasmussen, Inorg. Chem. 34 (1995) 1221.
[108] L. Glasser, in: W. Gans, A. Amann, J.C.A. Boeyens Jr. (Eds.), Fundamental Principles of Molecular Modeling, Plenum Press, New York, 1995.
[109] A. Gavezzotti (Ed.), Theoretical Aspects and Computer Modeling of the Molecular Solid State, vol. 1, Wiley, New York, 1997.
[110] D.A. Buckingham, L.G. Marzilli, A.M. Sargeson, J. Am. Chem. Soc. (1967) 5133.
[111] J.R. Gollogly, C.J. Hawkins, Inorg. Chem. 8 (1969) 1168.
[112] J.R. Gollogly, C.J. Hawkins, Inorg. Chem. 9 (1970) 576.
[113] J.R. Gollogly, C.J. Hawkins, Inorg. Chem. 11 (1972) 156.
[114] J.R. Gollogly, C.J. Hawkins, Aust. J. Chem. 20 (1967) 2395.
[115] J.-P. Mathieu, Ann. Phys. 19 (1944) 335.
[116] E.J. Corey, J.C. Bailar Jr., J. Am. Chem. Soc. 81 (1959) 2620.
[117] T.W. Hambley, G.H. Searle, M.R. Snow, Aust. J. Chem. 35 (1982) 1285.
[118] T.W. Hambley, G.H. Searle, Aust. J. Chem. 37 (1984) 249.
[119] A.M. Bond, T.W. Hambley, M.R. Snow, Inorg. Chem. 24 (1985) 1920.
[120] P. Comba, H. Jakob, B. Nuber, B.K. Keppler, Inorg. Chem. 33 (1994) 3396.
[121] P.V. Bernhardt, P. Comba, A. Mahu-Rickenbach, S. Stebler, S. Steiner, K. Várnagy, M. Zehnder, Inorg. Chem. 31 (1992) 4194.
[122] C.E. Schäffer, C.K. Jorgensen, Mol. Phys. 9 (1965) 401.
[123] C.E. Schäffer, Theoret. Chim. Acta 34 (1974) 237.
[124] E. Larsen, G.N. La Mar, J. Chem. Educ. 51 (1974) 633.
[125] M. Gerloch, J.H. Harding, R.G. Woolley, Struct. Bonding (Berlin) 46 (1981) 1.
[126] J. Glerup, O. Monsted, C.E. Schäffer, Inorg. Chem. 19 (1980) 2855.
[127] M. Gerloch, R.G. Woolley, J. Chem. Soc. Dalton Trans. (1981) 1714.
[128] L.G. Vanquickenborne, B. Coussens, D. Postelmans, A. Ceulemans, K. Pierloot, Inorg. Chem. 30 (1991) 2978.

[129] M. Gerloch, Comments Inorg. Chem. 18 (1996) 101.
[130] K Wüthrich, NMR of Proteins and Nucleic Acids, Wiley, New York, 1986.
[131] K. Wüthrich, Acc. Chem. Res. 22 (1989) 36.
[132] I. Bertini, A. Rosato, in: L. Banci, P. Comba (Eds.), Molecular Modeling and Dynamics of Bioinorganic Systems, Kluwer, Dordrecht, 1997, p. 1.
[133] L. Banci, Savellini, G. G, in: L. Banci, P. Comba (Eds.), Molecular Modeling and Dynamics of Bioinorganic Systems, Kluwer, Dordrecht, 1997, p. 191.
[134] T.W. Hambley, Inorg. Chem. 27 (1988) 2496.
[135] D. Ventur, K. Wieghardt, B. Nuber, J. Weiss, Z. Anorg. Allg. Chem. 551 (1987) 33.
[136] P. Hendry, A. Ludi, Adv. Inorg. Chem. 35 (1990) 117.
[137] A.W. Herlinger, J.N. Brown, M.A. Durger, S.F. Pavkovich, Inorg. Chem. 20 (1981) 2366.
[138] L.S. Magill, J.D. Korp, I. Bernal, Inorg. Chem. 20 (1981) 1187.
[139] D.H. Tempelton, A. Zalkin, H.W. Ruben, L.K. Templeton, Acta Crystallogr. 1335 (1979) 1608.
[140] R.J. Balahura, G. Ferguson, B.L. Ruhl, R.G. Wilkins, Inorg. Chem. 22 (1983) 3990.
[141] P. Comba, Inorg. Chem. 28 (1989) 426.
[142] R. Nagao, F. Marumo, Y. Saito, Acta Crystallogr. 1329 (1973) 2438.
[143] R.J. Geue, J. Hanna, A. Höhn, C.J. Qin, S.F. Ralph, A.M. Sargeson, A.C. Willis, in: S. Isied (Ed.), Electron Transfer Reactions, 1997, Ch. 8, p. 37. Advances in Chemistry Series 253, ACS, Washington DC, USA.
[144] H. Brunner, P. Hendry, A. Ludi (1998) unpublished results.
[145] A.A. Vlcek, Discuss. Faraday Soc. 26 (1958) 164.
[146] D.P. Rillema, J.F. Endicott, E. Papaconstanttinou, Inorg. Chem. 10 (1971) 1739.
[147] A.M. Tait, F.V. Lovecchio, D.H. Busch, Inorg. Chem. 16 (1977) 2206.
[148] R.L. Lintvedt, D.E. Fenton, Inorg. Chem. 19 (1980) 569.
[149] N.J. Curtis, G.A. Lawrance, A.M. Sargeson, Aust. J. Chem. 36 (1983) 1327.
[150] J. Sima, J. Labuda, Comments Inorg. Chem. 15 (1993) 93.
[151] (a) A.P.B. Lever, Inorg. Chem. 30 (1991) 1980. (b) A.P.B. Lever, Inorg. Chem. 29 (1990) 1271.
[152] H. Masui, A.B.P. Lever, Inorg. Chem. 32 (1993) 2199.
[153] E.S. Dodsworth, A.A. Vlcek, A.B.P. Lever, Inorg. Chem. 33 (1994) 1045.
[154] A.A. Vlcek, E.S. Dodsworth, W.J. Pietro, A.B.P. Lever, Inorg. Chem. 34 (1995) 1906.
[155] S. Lu, V.V. Strelets, M.F. Ryan, W.J. Pietro, A.B.P. Lever, Inorg. Chem. 35 (1996) 1013.
[156] Y.D. Gao, K.B. Lipkowitz, F.A. Schultz, J. Am. Chem. Soc. 117 (1995) 11932.
[157] D. Geselowitz, Inorg. Chem. 20 (1981) 4457.
[158] P.V. Bernhardt, P. Comba, T.W. Hambley, Inorg. Chem. 32 (1993) 2804.
[159] R.J. Geue, T.W. Hambley, J.M. Harrowfield, A.M. Sargeson, M.R. Snow, J. Am. Chem. Soc. 106 (1984) 5478.
[160] P. Gütlich, A. Hauser, H. Spiering, Angew. Chem. 106 (1994) 2109.
[161] P. Gütlich, Struct. Bonding 44 (1981) 83.
[162] H. Toftlund, Coord. Chem. Rev. 94 (1989) 67.
[163] K. Wieghardt, W. Schmidt, W. Herrmann, H.-J. Küppers, Inorg. Chem. 22 (1983) 2953.
[164] K. Wieghardt, H.J. Küppers, J. Weiss, Inorg. Chem. 24 (1985) 3067.
[165] J.C.A. Boeyens, A.G.S. Forbes, R.D. Hancock, K. Wieghardt, Inorg. Chem. 24 (1985) 2926.
[166] L.L. Martin, R.L. Martin, K.S. Murray, A.M. Sargeson, Inorg. Chem. 29 (1990) 1387.
[167] L.L. Martin, R.L. Martin, A.M. Sargeson, Polyhedron 13 (1994) 1969.
[168] P.V. Bernhardt, P. Comba, T.W. Hambley, G.A. Lawrance, Inorg. Chem. 30 (1991) 942.
[169] J. Peisach, W.E. Blumberg, Arch. Biochim. Biophys. 165 (1974) 691.
[170] J. Gazo, I.B. Bersuker, J. Garaj, M. Kabesokavá, J. Kohout, H. Langfelderová, M. Melník, M. Serátor, F. Valach, Coord. Chem. Rev. 19 (1976) 253.
[171] B.J. Hathaway, P.G. Hodgson, J. Inorg. Nucl. Chem. 35 (1973) 4071.
[172] J. Han, T.M. Loehr, Y. Lu, J. Selverstone Valentine, B.A. Averill, J. Sanders-Loehr, J. Am. Chem. Soc. 115 (1993) 4256.
[173] C.R. Andrew, H. Yeom, J. Selverstone Valentine, B.G. Karlsson, N. Bonander, G. van Pouderoyen, G.W. Canters, T.M. Loehr, J. Sanders-Loehr, J. Am. Chem. Soc. 116 (1994) 11489.
[174] A.S. Brill, Mol. Phys. 85 (1995) 727.
[175] C. Buning, P. Comba, M. Melter, work in progress.
[176] P. Comba, N.F. Curtis, G.A. Lawrance, M.A. O'Leary, B.W. Skelton, A.H. White, J. Chem. Soc. Dalton Trans. (1988) 2145.